Heightened Electromagnetic Fields between Metal Nanoparticles: Surface Enhanced Raman Scattering from Metal−Cytochrome *c*-Metal Sandwiches

Christine D. Keating, Kenneth K. Kovaleski, and Michael J. Natan*

Department of Chemistry, The Pennsylvania State University, University Park, Pennsylvania 16802

Received: June 22, 1998

This manuscript reports the demonstration of strong interparticle electromagnetic coupling in nanoparticle: molecule:nanoparticle sandwiches. These assemblies were prepared by adsorption of cytochrome *c* (Cc)-coated colloidal Au nanoparticles onto aggregated colloidal Ag. Surface enhanced Raman scattering (SERS) spectra for the Cc:Au conjugates (Ag:Cc:Au) were compared to those obtained by direct adsorption of Cc (Ag:Cc) at several visible excitation wavelengths. The use of identically prepared samples with the same effective [Cc] and the same laser power allows the effects of sample geometry and interparticle coupling to be probed. As expected, at all excitation wavelengths, Ag:Cc:Au gave less intense spectra than Ag:Cc, because (i) only a small percentage of the Cc molecules were close to the more SERS-active metal (Ag), and (ii) the heme, from which all observed vibrations arise, was oriented toward the Au, not the Ag. Nonetheless, the ratio of Ag:Cc:Au to Ag:Cc SERS intensity varied significantly with excitation wavelength, a phenomenon that can be accounted for only by a wavelength-dependent electromagnetic field. This, in turn, results from wavelength-dependent electromagnetic coupling between closely spaced colloidal Ag and colloidal Au. In addition to wavelength-dependent SERS intensity ratios, three separate lines of evidence support the existence of strong electromagnetic coupling: (i) the presence of a wavelength-shifted single particle surface plasmon band for Cc:Au conjugates upon exposure to agggregated Ag, (ii) demonstration of excitation wavelength-dependent photodriven conformational changes in Ag:Cc:Au, and (iii) dramatic increases in SERS intensities from protein−colloid conjugates prepared with Ag in place of Au.

Introduction

Since the discovery of surface enhanced Raman scattering (SERS)[1] in 1977,[2] there has been intense interest in the mechanisms responsible for the extraordinarily large enhancements in Raman signal observed for analytes adsorbed at appropriately roughened noble metal surfaces. Much of the observed enhancement can be accounted for by theory describing the electromagnetic fields at the metal surfaces,[3] the remainder being ascribed to chemical mechanisms.[4,5] Early SERS work showed that electrochemical roughening of Ag electrodes in the presence of analyte molecules increased enhancements, a result verified by more recent experiments.[6] This effect has been attributed to the entrapment of analyte molecules within the newly formed Ag nanostructures. SERS studies using evaporated and cold-deposited Ag films suggested that the molecules responsible for the observed signal are located in crevices or pores in the films.[7] In each system studied, it was postulated that the increased SERS signals resulted from the greatly enhanced electromagnetic (EM) fields that are possible between surface features.[6,7] Liver et al. have attempted to address this issue of "trapped" analytes using EM theory. They found that molecules in conical clefts (wedges) experienced no increase in EM field, while those between two spherical particles experienced greatly enhanced fields.[8] Theory suggests that, for spheroids completely covered with analyte, the molecules located between the two nanoscale metallic spheroids will experience the highest EM field, and thus the greatest SERS enhancement, while molecules which adorn the rest of the bispheroidal system will experience relatively weaker fields.[8,9] Difficulties achieving precise control over the nanoscale morphology of, and analyte placement at, SERS-active substrates has made experimental tests of these bispheroidal theories impractical.

We have prepared structures similar to the theoretical bispheroidal system, in which an analyte molecule is positioned between two noble metal particles. This has been accomplished by preparing protein:colloidal Au conjugates[10] and adsorbing them to (SERS-active) colloidal Ag aggregates.[11] The Ag aggregates are composed of discrete, nanometer-scale spheroidal and ellipsoidal particles, and comprise the main substrate for enhanced scattering. The Au particles used are monodisperse, 12-nm diameter spheres better suited for conjugation with biomolecules[10−14] than for use as SERS substrates. Biomolecule:colloid conjugates[11] are prepared by coating these 12-nm diameter Au nanoparticles with the heme-containing protein, cytochrome *c* (Cc).[15] Upon adsorption of the Cc:Au conjugates to aggregated colloidal Ag, a portion of the protein molecules are "trapped" between the Ag and Au particles (Chart 1). This "sandwich" approach has several attractive features. (i) Two colloidal metal particles can be placed a known distance apart, namely the protein diameter. (ii) The choice of Au and Ag particles allows electromagnetic coupling to be clearly identified through wavelength-dependent measurements of SERS spectral intensities. (iii) Rigid encapsulation of the heme chromophore in the protein allows for better control of adsorption and orientation than for small-molecule analytes. (iv) Since the heme group is bound within the protein structure and does not directly contact the surface, chemical enhancement mechanisms should

* To whom all correspondence should be directed (e-mail: natan@chem.psu.edu).

10.1021/jp982724r CCC: $15.00
Published on Web 11/03/1998

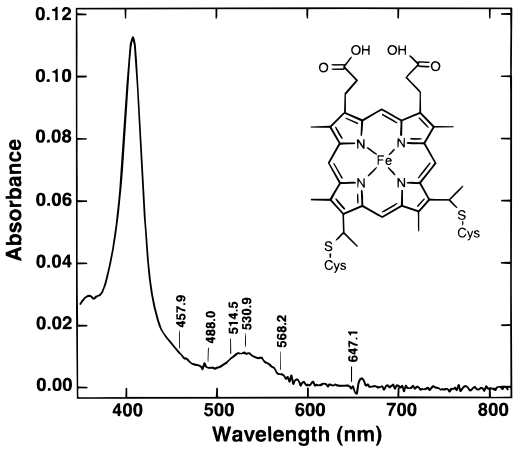

Figure 1. Optical spectrum for horse heart ferricytochrome *c*, illustrating the wavelengths of several of the laser lines used for excitation of Raman scattering. Inset: chemical structure of the heme group.

CHART 1: Schematic Representation of Two Geometries for Cc SERS on Aggregated Ag

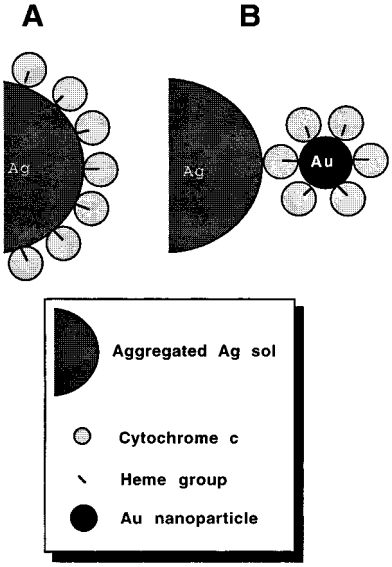

not be important for this system. Importantly, the sandwich geometry (i.e., **B** in Chart 1) can be compared experimentally to the geometry in which the colloidal Au is absent [i.e., directly adsorbed Cc (**A** in Chart 1)].

Cytochrome *c* (Cc) was chosen for the present study because of the large amount of work that has appeared in the literature describing its vibrational spectra (both solution resonance Raman[16] and resonant SERS[17−19]) and adsorption at several types of surfaces.[17,20] The optical spectrum of ferricytochrome *c* (Figure 1) shows the intense Soret band at 408 nm ($\epsilon = 10^5$ M^{-1} cm^{-1}) and a weaker absorbance due to the Q-bands, which are centered at ~532 nm ($\epsilon \sim 10^4$ M^{-1} cm^{-1}).[15,16] Excitation into these absorbance bands leads to resonance enhancement of Raman scattering from vibrational modes coupled to the electronic transitions (which can yield an additional several orders of magnitude in enhancement over those observed for nonresonant SERS). Moreover, the location and orientation of the heme group within Cc are known. Since SERS enhancements decrease sharply with distance from the metal surface,[1,21−23] these factors are very important; in Cc, they are favorable for SERS investigations. Specifically, the heme of Cc is very near the surface of the protein, at a cleft rich in positively charged surface lysine residues,[15] and since the surfaces of metal nanoparticles are negatively charged,[24] this lysine-rich patch binds to the metal surface. The heme group is thought to be held at an angle of approximately 45° with respect to the metal surface in this geometry[16,20] (a far more favorable orientation for SERS enhancement than one with the heme group parallel to the surface).[25] In addition, a second, weaker region of positive charge exists on the opposite side of Cc, facilitating sandwich formation.

Previous studies have described resonant SERS (SERRS) of proteins at aggregated, citrate-reduced Ag sols similar to those employed here. Such surfaces have been shown to be nondenaturing for Cc,[17,18] chlorcatechol dioxygenase,[26] and several cytochromes P450.[27] These sols are thought to have an adsorbed layer of citrate ions, which controls protein adsorption and prevents unfavorable interactions between the biomolecules and the Ag surface.[27] Citrate-reduced *Au* sols are not commonly used as SERS substrates; however, conjugates of colloidal Au and biomolecules are popular as electron-dense markers for TEM staining of biological tissues.[10] In this context, retention of activity has been demonstrated for many Au-bound biomolecules.[10,12] In the present study, the wavelength dependence of SERS from Cc directly adsorbed to aggregated colloidal Ag (Ag:Cc, Chart 1, **A**) is compared to that for Cc:Au conjugates adsorbed to aggregated Ag sol (Ag:Cc:Au, Chart 1, **B**).[28] Note that, as described in the previous paper, the heme group ends up in close proximity to the *first* metal particle to which it is exposed. Thus, the distance between the Cc heme group and the Ag surface is much larger in **B** than that in **A**.

Aggregates of Ag and Au nanoparticles can both serve as substrates for SERS, although the former typically give higher enhancements.[1] Citrate-reduced colloidal Ag has long been a favorite SERS substrate, due to its ease of preparation, good biocompatibility (as compared to BH_4-reduced sols and roughened Ag electrodes) and high SERS enhancements.[17,18,29,30] Typical citrate-reduced Ag sols are polydisperse, and contain spherical and spheroidal particles as well as long rods and several varieties of three-dimensional polygons.[31] It has been suggested that the enhancements from this sol arise almost entirely from molecules adsorbed at a small number of "hot" spheroids ("hot" particles were found to be very large, ≥100 nm).[29] Colloidal Au nanoparticles, in contrast, can be prepared by citrate reduction to yield highly monodisperse solutions of nearly spherical particles.[10,32,33] These sols are not as enhancing for SERS, due in part to the less optimal particle sizes/shapes and in part to the less favorable electromagnetic properties of Au as compared to Ag.[34] In general, Raman scattering is proportional to ω^4, where ω is the frequency of the exciting laser line.[35] While this is also true for SERS, it has been observed that excitation into the surface plasmon absorption band of metallic substrates gives rise to the greatest enhancements, an effect that can overpower the ω^4 dependence.[1,36] For the experiments described here, Ag sols have been aggregated prior to SERS spectral acquisition. This has the effect of greatly increasing SERS enhancements and altering the extinction spectrum such that a very broad collective plasmon oscillation absorbance appears, making excitation of this band possible at nearly all visible wavelengths. For Au sols, however, strong damping of the Au nanoparticle surface plasmon occurs at energies above ~2.2 eV (which corresponds to wavelengths below ~560 nm),[34,36c] and high SERS enhancements at Au surfaces have only been observed using red excitation.[1,37] Thus, the SERS excitation profiles for the two metals are readily distinguishable.

In this article we report surface-enhanced Raman scattering spectra at aggregated colloidal Ag sols for Cc:Au and Cc:Ag nanoparticle conjugates (i.e., Ag:Cc:Au and Ag:Cc:Ag, respectively),[28] as they compare to SERS spectra for directly adsorbed Cc (i.e., Ag:Cc). By acquiring SERS spectra for Ag:Cc and Ag:Cc:Au (or Ag:Cc:Ag) under the exact same conditions, it has been possible to eliminate effects not due to the geometry of the samples. On the basis of the location of the Cc heme group, in close proximity to the Ag surface for directly adsorbed Cc, but far-removed from the surface in sandwiches, it was anticipated that Ag:Cc:Au would yield far less intense spectra at all excitation wavelengths. This behavior was found using 488.0-, 514.5-, or 647.1-nm excitation. However, when excited with 568.2 nm light, spectra for Ag:Cc:Au and Ag:Cc were of comparable intensity. This anomalous wavelength dependence results from simultaneous resonant excitation of the Ag aggregate, the Cc heme, and the colloidal Au nanoparticle, indicating that interparticle electromagnetic coupling between Cc-separated Au and Ag nanoparticles is large. Further evidence for strong interparticle coupling comes from UV−vis spectra that show a strongly shifted surface plasmon band for Cc:Au conjugates upon exposure to aggregated Ag and from photoinduced conformational changes in Ag:Cc:Au that occur at 568.2-nm excitation but not with 514.5-nm excitation. Moreover, at excitation wavelengths where Cc absorbs, SERS spectral intensities for Ag:Cc:Ag significantly exceed those for Cc:Ag. Exploitation of this strong electromagnetic coupling via deliberate preparation of nanoparticle:analyte:nanoparticle sandwiches is an exciting new approach to sensitive SERS measurements.

Experimental Section

Materials. Horse heart cytochrome *c* (Sigma) was purified by affinity chromatography according to a literature protocol.[38] Poly(ethylene glycol) (MW 20 000) was from Fluka. All other reagents were acquired from one of the following suppliers: J. T. Baker, Aldrich, Acros, Sigma, VWR, and used without further purification. Horseradish peroxidase (type VI-A) was from Sigma. All H_2O was 18.2 MΩ, from a Barnstead Nanopure system. The pH of colloid solutions was determined using pH test strips (colorpHast) to within ±0.5 pH unit.

Preparation of Colloidal Au and Ag Nanoparticles. Ag sols were prepared by aqueous reduction of $AgNO_3$ with Na_3-citrate following the method of Lee and Meisel.[39] Ag sols prepared in this way are polydisperse, with average particle diameters typically ∼30 nm and standard deviation ∼25 nm.[31] Colloidal Au 12 nm in diameter colloidal Au was prepared by the citrate-reduction of $HAuCl_4$ as previously described.[32,33] Particles referred to in the text as "12 nm diameter Au" were nearly spherical, with standard deviations <1.5 nm. Several preparations were used in this work. For each, particle sizes were determined from transmission electron microscopy (TEM) micrographs as described previously.[33]

Particles referred to as "40 nm" were prepared by using 12-nm Au particles as "seeds" for nucleation of larger particles,[40] as were Ag-coated Au particles (henceforth "Ag/Au"). Preparation of both types of "seeded" particles is described elsewhere.[40,41] The concentration of Ag/Au nanoparticles in this solution was calculated to be $\sim 4 \times 10^{-11}$ M, based on the initial concentration of 12-nm Au "seed" particles.

EDTA-reduced Ag sols were prepared according to Rospendowski et al.[27] using the following procedure. H_2O (100 mL) was brought to boil with rapid stirring. To this, 1.0 mL of 0.1 M EDTA and 4.0 mL of 0.1 M NaOH were added at once, followed by 1.3 mL of 0.1 M $AgNO_3$. The solution was boiled for 60 s, after which 300 μL of 0.1 M HCl was added and the solution was kept boiling and stirring for 2−3 min. The resulting solution was a bright yellow color; a 7% aqueous solution gave an absorbance of 1.43 at λ_{max} (408 nm). TEM analysis of this colloid showed the presence of 14-nm (±8 nm) diameter Ag nanoparticles.

Preparation of Cc:Au Conjugates. Cc:Au colloid conjugates were prepared using horse heart ferricytochrome *c* and 12-nm diameter colloidal Au as described previously.[11] Cc:Au samples were stable for several months when stored at 4 °C, when prepared with 12-nm diameter particles [Cc:Au, to distinguish them from conjugates made with 40-nm diameter Au(40) or 60-nm diameter Au(60) particles].

Preparation of HRP:Au Conjugates. Protein:Au colloid conjugates were prepared using horseradish peroxidase (HRP) and 12-nm diameter colloidal Au. The binding of HRP to colloidal Au particles was followed by a flocculation assay.[10−12] Conjugates were then prepared by addition of 100 μL of 9.7 mg/mL HRP to 1.20 mL of 14 nM, 12-nm Au particles. The solution was mixed gently and allowed to react for 15 min before centrifugation in a Fisher Scientific Micro Centrifuge Model 235C for 15 min at 13 600*g*. The supernatant was removed and the (soft) pellet resuspended in H_2O.

Cc:Au(40) Conjugates. As-prepared 40-nm Au solutions were calculated to be 0.405 nM in particles, based on the assumption that all Au particles in the final solution were formed by growth of 12-nm "seed" particles. The narrow size distribution seen in TEM analysis of seeded colloid validates this assumption.[40b] The stabilizing concentration of Cc for 40-nm Au was determined by a flocculation assay, as described for 12-nm Au. A large excess (470%) of this value was added to the colloidal solution to prepare Cc:Au(40) conjugates, which were then incubated for 15 min and centrifuged 30 min at 13600*g*. The supernatant was removed and the (soft) pellet resuspended in H_2O. Cc concentration in these samples prior to centrifugation/resuspension was 3.64×10^{-7} M.

Cc:Au(60) Conjugates. Particles referred to as "60 nm" in the text were purchased from Goldmark Biologicals (Phillipsburg, NJ). Literature supplied by Goldmark Biologicals listed the particle diameter as 62.8 nm, the concentration as 2.6×10^{10} particles/mL (43.2 pM in particles), and claimed a coefficient of variation in particle diameter of <20%. Our transmission electron micrographs of these particles support the diameter and coefficient of variation listed and indicate that the particles are quite spherical. In addition, a polymeric stabilizer could be observed in TEM images; this material did not appear to impact flocculation, conjugate formation, or SERS spectra. A calculation for the number of Cc molecules necessary to completely coat 62.8-nm Au particles gave ∼1500 Cc molecules per Au particle. Flocculation data indicated that about 20% more than this value was required. This excess could be accounted for by accumulated errors in particle concentration, particle diameter, and Cc "footprint" on Au. Conjugates were incubated for 15 min, then spun 10 min at 13600*g*. Because the particles were so dilute, only very weak signal could be observed from conjugates resuspended in 1.25 mL; thus, conjugates were resuspended in 100 μL H_2O. Cc concentration in these samples prior to centrifugation/resuspension was 1.45×10^{-7} M.

Cc:Ag-Coated Au Conjugates. Cc:Ag/Au conjugates were prepared in a similar fashion. The saturating [Cc] was determined by flocculation assay, after which either 21% or 110% of this value of Cc was added to a colloidal solution at

pH 9.5 ± 0.5. Cc:Ag/Au was purified by centrifugation and resuspension in H_2O. Some aggregation (evidenced by a color change from yellow/brown to a cloudy orange/brown color) was observed within 2 min of resuspension of conjugates, after which no further change was observed. All SERS spectra were acquired after this color change occurred.

Cc:Ag Conjugates. Due to the inherent instability of citrate-reduced Ag sols, it proved difficult to prepare Cc:Ag conjugates using these particles. For this reason, EDTA-reduced colloidal Ag was chosen for preparation of Cc:Ag. Conjugates were prepared by addition of 110% of the stabilizing concentration of Cc, as determined from flocculation studies (carried out as for Au). Thus, 50 μL of 10 μM Cc was added to 1.2 mL of Ag nanoparticles at pH 9.5 ± 0.5. The resulting solution was incubated for 15 min, then centrifuged at 13600*g* for 15 min and resuspended in 1.25 mL of H_2O.

SERS Acquisition. SERS instrumentation and sample preparation are described in the accompanying article in this issue.[11]

Results and Discussion

Sample Geometry. The morphology of colloidal metal aggregates has been investigated by several groups and has been shown to include long stringlike chains and/or fractal structures.[1,42] In Chart 1, aggregated, polydisperse colloidal Ag is depicted as a single particle. While this is a gross oversimplification, Chart 1 nevertheless accurately depicts the three key differences between **A** (Ag:Cc) and **B** (Ag:Cc:Au). First, the heme groups are oriented away from the Ag particle in **B** and toward it in **A**. This is because the lysine-rich heme pocket of Cc[15] is attracted to the negatively charged metal particles; it is expected to bind with the heme closest to the first type of metal nanoparticle it encounters. Thus, the heme will be oriented close to the Ag surface when Cc is added directly to Ag sols; indeed, this is why it has proven simple to obtain SERS spectra of Cc adsorbed to Ag. However, the heme will be oriented toward the Au surface for Ag:Cc:Au samples. As a result, the distance between the SERS-active Ag particle aggregate and the heme moiety is significantly greater for Ag:Cc:Au (**B**) than for Ag:Cc (**A**). The other two differences between **A** and **B** relate to the geometric relationship between the protein and the metal particles. In **A**, while every molecule of Cc is in close proximity to the aggregated Ag, in **B** most Cc molcules are *not* close to the Ag surface, and some are separated by more than 12 nm, the diameter of the Au particle. Moreover, while there certainly can be geometries of **A** in which Cc is in a crevice between two particles, only in **B** will Cc's be found between different metals (Au and Ag). The easily differentiable SERS behavior of these metals is a logical starting point for investigation of the optical properties of these metal nanoparticle:Cc:metal nanoparticle sandwiches.

Colloidal Ag:cytochrome c:12-nm Diameter Au Sandwiches. An optical spectrum for horse heart ferricytochrome *c* is shown in Figure 1. Several wavelengths corresponding to SERS excitation wavelengths used in this work are indicated on the spectrum. When λ_{ex} coincides with an electronic transition, resonant enhancement of the Raman scattering can occur. Some of the excitations used in this work are in the region of the Q-bands (~500−580 nm), while others do not coincide with any electronic transitions of the heme chromophore.

Figure 2 compares SERS spectra obtained for each of the geometries in Chart 1 at several excitation wavelengths. The upper spectrum in each part is that for Cc adsorbed directly to the Ag surface (**A**, dotted lines), while the lower spectrum corresponds to adsorbed Cc:Au conjugates (**B**, solid lines). In these experiments, not only are cytochrome *c* concentrations, sample volumes, excitation wavelengths, light collection geometries and efficiencies, and integration times identical for **A** and **B** in each part,[43] but so are any effects due to resonance enhancement of Cc's heme or to the wavelength-dependence of SERS from Ag aggregates. Thus, comparison of spectra for **A** and **B** for each set of conditions allows effects not due to nanoparticle-protein geometry to be factored out.

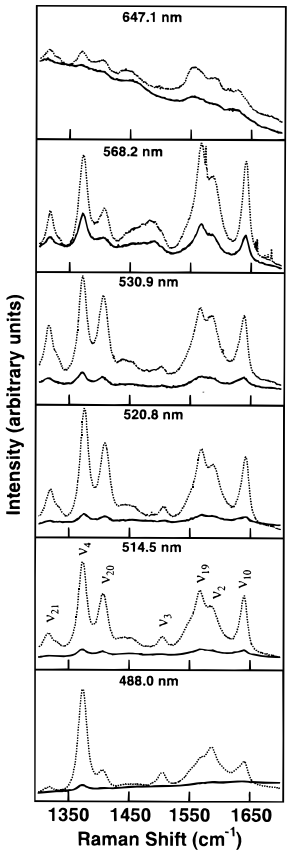

Figure 2. SERS spectra, at aggregated Ag sol, for cytochrome *c* (···) and cytochrome *c*:Au colloid conjugates (—) at, from top to bottom, the following excitation wavelengths (laser powers, integration times): 647.1 nm (170 mW, 30 s), 568.2 nm (54 mW, 30 s), 530.9 nm (47 mW, 30 s), 520.8 nm (50 mW, 15 s), 514.5 nm (55 mW, 30 s), and 488.0 nm (142 mW, 15 s). [Cc] = 6.8×10^{-8} M. Each spectrum shown is the average of three accumulations for the same sample. The spectrum for 514.5-nm excitation shows assignments for Cc vibrational modes.[16]

The spectra shown in Figure 2 are due to vibrations of the heme moiety of Cc and agree well with previous resonant-SERS studies of Cc on Ag sols at high Cc coverage.[17] Band assignments are given in Table 1. The position of the oxidation state marker band (ν_4) at ~1375 cm^{-1} indicates that the Cc exists in the Fe^{3+} state,[16] which was expected since the Cc used in these studies was ferriCc prior to adsorption to Ag. In addition, the location of the spin state marker band (ν_{10}) at ~1635 cm^{-1} indicates that the Cc Fe is low-spin,[16] meaning that it has not undergone ligand loss, transforming to the high-spin state (a sign of denaturation or other conformational change due to surface adsorption). The data shown here are similar to those reported by MacDonald and Smith[17] for Cc SERS at aggregated Ag sols (λ_{ex} = 514.5 nm) and do not show signs of the surface-induced conformational changes observed by Hildebrandt and co-workers (note that, at this resolution, only relatively large conformational changes would be easily detectable).[18] In

TABLE 1: Frequencies and Assignments for Cc−Heme Vibrations

488 nm		514.5 nm		568.2 nm		647.1 nm		assignment
A	B	A	B	A	B	A	B	(ref 16)
		1316		1313	1313	1316	1317	ν_{21}
1373		1375	1376	1369	1368	1368	1368	ν_4
1402		1407	1404	1403	1404	1404	1404	ν_{20}
		1450	1455			1444	1441	
				1487	1487			*a*
1502		1505						ν_3
1556	1558	1565		1561	1562	1555	1556	ν_{11}
1587		1585		1580	1579	1585	1585	ν_{19}
						1611	1611	
						1627	1627	*b*
1637		1640	1641	1636	1637			ν_{10}

[a] Although this band is in the general region for high-spin ν_3, it is only present with 568.2-nm excitation, and identically prepared samples excited at other wavelengths give ν_3 at 1503 cm^{-1} (indicative of low-spin Fe); we find it unlikely that ν_3 moves to 1487 cm^{-1} only at λ_{ex} = 568.2 nm, especially given that the other spin state marker bands all indicate low-spin Fe. Thus, we have left this band unassigned. [b] The position of ν_{10} at 1627 cm^{-1} observed for λ_{ex} = 647.1 nm would indicate that the heme has undergone a spin-state conversion to a high-spin Fe. Again, this seems unlikely to have occurred for only one excitation wavelength; thus, we have not assigned the 1627 cm^{-1} band as ν_{10}.

summary, the Cc giving rise to the observed SERS signals appears to be in its native conformation.

While the critical comparisons are between spectra for Ag:Cc and Ag:Cc:Au (i.e., **A** and **B**), it is useful to begin discussion of the SERS wavelength dependence by looking at each component separately. For the Cc directly adsorbed at Ag (**A**, dotted lines), significant differences in relative peak intensities for SERS spectra excited at different wavelengths are observed. These differences in relative intensities cannot be explained in terms of protein concentration (all samples were identically prepared); however, they are similar to ratios previously observed in Cc solution resonance Raman (RR) excitation profiles and SERS enhancement profiles for free Fe(III) protoporphyrin at Ag electrodes.[16,44] Excitation at 514.5 and 568.2 nm gives rise to intense signal due to resonant SERS, while excitation at 488.0 or 647.1 nm, which do not coincide with electronic transitions of the heme, required much higher laser powers and led to a weaker signal attributable to nonresonant SERS.

Inspection of Figure 2 also reveals differences in the relative intensities of the various bands for the different λ_{ex}. For example, at 488.0-nm excitation, the ν_4 vibration dominates the spectrum, while at λ_{ex} = 568.2 nm, ν_4, ν_2, and ν_{10} have roughly equal intensities. In RR experiments, modes with A_{1g} symmetry (ν_4, ν_3) are known to be preferentially enhanced by excitation into the Soret band (Franck−Condon, or A-term scattering mechanism), while excitation into the Q-bands (vibronic, or B-term scattering) favors the nontotally symmetric modes (B_{1g}, A_{2g}, B_{2g}), resulting in greater signal from ν_{10}, ν_{19}, and ν_2 vibrations.[18,45] For the Cc SERS data in Figure 2, excitation at 488.0 nm, although not resonant with the Soret band, results in greater enhancement of ν_4, while excitation into the Q-bands leads to a relative increase in signal from the other bands. At 647.1-nm excitation, ν_4 is much diminished compared to the other bands. Thus it appears that even for preresonance, excitation wavelengths closer to the Soret band (488.0 nm) favors A-term scattering, while excitations further to the red favor B-term scattering.

Based on the much greater distance between the heme and the Ag surface in the Ag:Cc:Au samples, a substantial decrease in signal in the Ag:Cc:Au samples (**B**) vs the Ag:Cc samples (**A**) is expected. To a first approximation, SERS EM enhancement is predicted to go as $(r/r+x)^{12}$, where r is the radius of curvature of the surface feature on the enhancing surface and x is the distance from the surface to the analyte.[1] The aggregated colloidal Ag surface is highly irregular, making estimates of r difficult; we will use the average radius of a single Ag particle (r = 150 Å) as a rough approximation. The Cc is ~34 Å in diameter,[46] with the heme group located close to one side. If we assume the heme group is located 3 Å from the surface and is 12 Å across, then x (the distance to the edge of the heme group) = either 3 Å (geometry **A**) or 19 Å (geometry **B**). Substituting into the distance dependence equation gives a factor of 3.4 difference in expected enhancement factor between the two orientations. For Ag:Cc:Au (**B**), this calculated distance effect is valid for only those Cc molecules located directly between the Ag surface and the Au particle; in fact, most of the Cc molecules are located significantly farther from the Ag surface. Enhancement factors for the Cc on the far side of the Au nanoparticle (x = 150 + 34 + 120 + 3 Å) is expected to be *3 orders of magnitude* lower than for the Cc in geometry **A**, assuming no contribution from the Au particle. Furthermore, the selection rules for SERS dictate that the efficiency of scattering will be affected by the angle between the heme and the surface,[25] meaning that not all Cc molecules around the Au particle will be equally enhanced. Thus, one might not expect to observe Ag:Cc:Au SERS *at all*, based on distance arguments.

The lower spectra in each part of Figure 2 are SERS for Cc:Au conjugates adsorbed to aggregated Ag sols (**B**). Ag:Cc:Au spectra are very weak as compared to Ag:Cc at the same [Cc] and acquisition parameters, but nevertheless observable. The wavelength dependence for Cc:Au on aggregated Ag might be expected to mirror that observed for Cc on Ag; optimum signal would be predicted from 514 to 568 nm, where benefit from resonant excitation of the heme chromophore could be realized.[16] However, the SERS data show optimum scattering from Cc:Au at 568.2-nm excitation; at this wavelength, the signal for Cc:Au approaches that for Cc. Excitation at shorter wavelengths (e.g., 514.5 nm) leads to much poorer signal for Cc:Au, despite good SERS for directly adsorbed Cc at these wavelengths. The anomalously high SERS intensity observed with 568.2-nm excitation cannot result from the wavelength-dependence of SERS at Ag aggregates (since this is unchanged between **A** and **B**). Likewise, all other variables except for the particle-molecule geometry are the same between Ag:Cc:Au and Ag:Cc samples.

Both the apparent relaxation of the SERS distance dependence at 568.2 nm and the difference in **B** vs **A** excitation profiles can be explained by the optical properties of Au nanoparticles: 568.2 nm is, and 514.5 nm is not, a wavelength at which heme molecular vibrations *and* Au surface plasmon polaritons can be resonantly excited simultaneously. That large SERS enhancements are observed under this condition suggests that the Au nanoparticles are taking part in enhancement of Raman scattering from Cc heme vibrations (further evidence will be described below). At shorter wavelengths, the damping of the Au plasmon diminishes this effect substantially, leaving the (distant) aggregated Ag substrate as the sole source of enhancement for the heme. Note that the optical properties of the Au nanoparticles alone cannot explain the magnitude of the observed scattering. A Raman spectrum of Cc:Au alone in solution shows negligible signal, even at a 10-fold greater concentration of Cc:Au conjugate and with 8-fold longer integration time (Supporting Information). Clearly, both the Au and Ag surfaces play important roles in the observed SERS spectra.

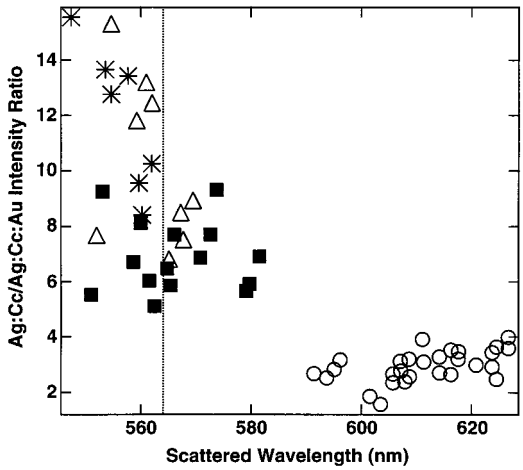

Figure 3. Ag:Cc to Ag:Cc:Au intensity ratio for ν_4 as a function of the wavelength of scattered light from each of several vibrational modes. These data were calculated from the spectra shown in Supporting Information. Excitation wavelengths: 514.5 (*), 520.8 nm, (△); 530.9 nm, (■); 568.2 nm, (○). The dotted line serves to guide the eye.

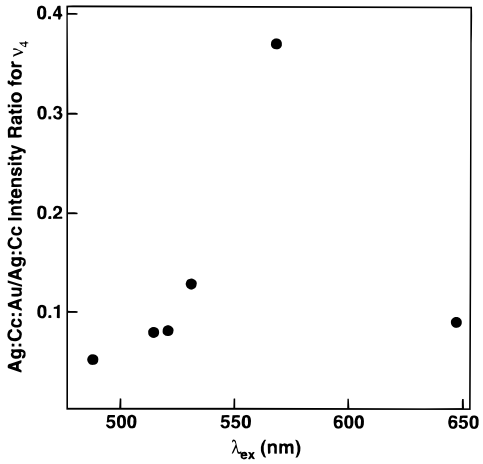

Figure 4. Ag:Cc to Ag:Cc:Au intensity ratio for ν_4 band versus excitation wavelength.

One reason that SERS enhancements are in general so large is that heightened electric fields at SERS-active substrates act on both incoming and scattered photons. However, since the scattered light is shifted from the incident frequency by the amount of the vibrational frequency, the incident and scattered radiation may not be equally surface enhanced. The large number of strong vibrational modes present in Cc SERS spectra make it possible to compare the relative SERS enhancements for Cc:Au and Cc at aggregated Ag sols over a range of scattered wavelengths (λ_s). SERS spectra for Cc and Cc:Au at aggregated Ag for $\lambda_{ex} = 514.5$, 520.8, 530.9, and 568.2 nm were used to make a plot of Ag:Cc to Ag:Cc:Au intensity ratio vs λ_s, shown in Figure 3 (full spectra are available as Supporting Information). Use of such a ratio factors out any differences between samples due to Cc concentration, laser power, collection optics, resonant enhancement of the heme moiety, wavelength-dependent SERS from the Ag aggregates (all of which should be the same for Cc and Cc:Au samples), or any other effects constant between samples. In Figure 3, each λ_{ex} is represented by a separate symbol. Exhibiting the lowest ratios, 568.2 nm (circles) is the optimal λ_{ex} for all vibrational modes of Cc:Au (relative to Cc). There does not appear to be much variation in the intensity ratio for different vibrations at this λ_{ex}, despite an ~40 nm wavelength range for the vibrational modes. For $\lambda_{ex} = 530.9$ (squares), 520.8 nm (triangles), and 514.5 nm (asterisks), there is more scatter in the data, due to poorer signal for Ag:Cc:Au. However, several trends are evident. First, while the scattering excited by excitation at 568.2 and 530.9 nm is insensitive to scattering wavelength (λ_s), that excited at 520.8 or 514.5 nm appears to be strongly dependent on λ_s. Why should only some excitation wavelengths lead to λ_s-dependent scattering ratios? One explanation is that, in fact, all are λ_s-independent, and the apparent slope in the 514.5- and 520.8-nm data simply reflects the poorer signal-to-noise ratio for Ag:Cc:Au at these exitations, coupled with the lesser intensity of lower cm^{-1} vibrations in Cc spectra and the further decrease in the intensity of these low wavenumber bands with shorter λ_{ex}. However, although the signal-to-noise ratio for the spectra used to calculate these ratios was less than for the corresponding 568.2- and 530.9-nm spectra, it was not sufficiently lower to easily account for the steep slope observed in the $\lambda_{ex} = 520.8$- and 514.5-nm ratios. An alternate, more likely explanation for the data shown in Figure 3 is that, for 568.2- and 530.9-nm excitation, there is little difference between incident and scattered light from the standpoint of enhancement, while at 520.8- and 514.5-nm excitations, there is so little enhancement of the incident light that any slight increases due to red shifting (for the scattered light) are observable. Whatever the explanation for these results, there is clearly a wavelength dependence to λ_{ex} (and possibly to λ_s for short λ_{ex}). These data comprise further evidence that the wavelength-dependent optical properties of the Au nanoparticles (to which Cc is bound) are impacting the outcome of SERS experiments.

Cc vibrational modes are highly sensitive to many factors, including the conformational state of the protein. Small changes in the average geometry of adsorption of Cc to colloidal Ag can lead to measurable changes in relative peak intensities. To avoid any complication in Ag:Cc:Au vs Ag:Cc intensity ratio data due to slight differences in Cc orientation for the two geometries, the ratios were plotted vs λ_{ex} for a single vibrational mode (ν_4). The ν_4 band was chosen because it is relatively insensitive to changes in protein conformation.[16−17] A plot of the Ag:Cc:Au to Ag:Cc (i.e., **B**/**A**) intensity ratio for the ν_4 band versus excitation wavelength is shown in Figure 4 (note the inversion of this ratio as compared to the **A**/**B** ratio shown in Figure 3; for the remainder of the paper **B**/**A** ratios will be used, such that larger ratios correspond to larger relative signal for the sandwich geometry **B**). This ratio is less than 1 at all λ_{ex}, reflecting the weak relative signal of Ag:Cc:Au as compared to Ag:Cc. Changes in the ratio are observed with λ_{ex}, indicating that the SERS enhancement profiles for the two samples are not the same. The **B**/**A** intensity ratio increases monotonically from 488.0 to 568.2 nm, as the signal from Cc:Au increases relative to that of Cc alone. This mirrors the trend shown in Figure 3, and can be explained by the diminishing effects of plasmon damping for Au as wavelength increases. The **B**/**A** ratio decreases again as λ_{ex} lengthens to 647.1 nm. This excitation wavelength is not in resonance with the heme, but this is the case for *both* samples. Since the Au surface plasmon is less damped at 647.1 nm than at 568.2 nm,[34] one might have expected a larger value for this ratio; the falloff can be understood upon consideration of the optical properties of these SERS samples.

SERS on aggregated metal colloids is highly dependent upon the absorbance properties and aggregation state of the particles.[1,36] The optical spectrum of Cc:Au conjugates (Figure 5, top part) is essentially unchanged from that of the 12-nm diameter Au particles used in their preparation. A maximum at ~520 nm is present, due to the surface plasmon absorbance

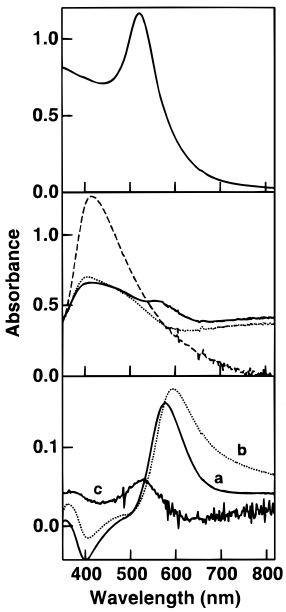

Figure 5. Top: Optical spectrum for Cc:Au conjugates. Middle: Optical spectra for unaggregated Ag sol (—), diluted 1:4.3 with H_2O) and for SERS samples consisting of aggregated Ag sol with Cc (•••) and with Cc:Au (—). Aggregated samples were prepared as described for SERS samples in the Experimental Section and then diluted 1:4.3 with H_2O. Bottom, difference spectra for several SERS samples minus the spectrum for the aggregated Ag sol alone: (a) Cc:Au, (b) unconjugated 12-nm Au, and (c) HRP:Au.

of the particles. Optical spectra for the citrate reduced Ag sol used in this work, and for Ag:Cc and Ag:Cc:Au SERS samples are also shown in Figure 5 (middle part). Aggregation of the Ag sol results in decreased extinction at λ_{max} (~405 nm) and increased extinction at longer wavelengths. This is due to the replacement of single-particle plasmon oscillations by collective-particle oscillations, which occur at longer wavelengths. The broadness of these features indicates the presence of many different types of aggregates in the solution. Nevertheless, there is a clearly discernible shoulder between 550 and 600 nm for the Ag:Cc:Au sample that is not present in the Ag:Cc sample. (It should be noted here that it *is* possible to distinguish Ag:Cc:Au and Ag:Cc SERS samples by eye, the former being slightly purplish). A subtraction optical spectrum for the Ag:Cc:Au SERS sample minus an aggregated Ag "blank" (Ag:Cc:Au−Ag) is shown in the lower part of Figure 5 (curve a, —). Here the absorbance giving rise to the shoulder in the middle part can be readily distinguished as a peak with $\lambda_{max} = 574$ nm. This feature is only observed when Cc:Au conjugates are present in the sample, and the peak is significantly redshifted relative to the λ_{max} for Cc:Au conjugates alone in solution (Figure 5, top part). Proximity to the aggregated Ag surface could account for shifting the Cc:Au λ_{max} to longer wavelengths. Thus, it appears that the data shown in Figure 4 are reporting on the optical spectrum for the Ag:Cc:Au sandwich under interrogation in the SERS experiment, as distinct from the Ag aggregates as a whole or from the Cc:Au conjugates alone. Note that it cannot be expected that bulk optical properties (as measured by UV−vis) and the local optical properties at the sites giving rise to SERS scattering would necessarily be the same or even similar; nonetheless, in this case the SERS and absorbance spectra appear to be reporting on the same species. The data shown here cannot be accounted for without electromagnetic coupling between the Ag aggregates and the protein-coated Au particles; hence both must be participating in the observed enhancements. Indeed, the optical difference spectrum for uncoated Au (Figure 5, bottom part, curve b, •••) is similar to that for Cc:Au, except that the λ_{max} is redshifted even further, indicating an even greater degree of coupling between the Au particles and the Ag aggregates. This result is reasonable given the closer approach possible without the protein coating between the Au and Ag particles.

Much less coupling is observed upon replacing the Cc:Au conjugates with horseradish peroxidase:Au conjugates (HRP:Au). The optical difference spectrum for a SERS sample containing HRP:Au conjugates minus that of the Ag aggregate blank is also shown in the bottom part of Figure 5 (curve c). Even though the concentration of Au nanoparticles in all three samples for which difference spectra are shown in Figure 5 are essentially the same, the absorbance of the Ag:HRP:Au−Ag is noticeably smaller. More importantly, it is essentially unshifted relative to the free conjugates with a $\lambda_{max} = 528$ nm (in addition, curve c is nearly identical to the optical spectrum for the same concentration of uncoated Au nanoparticles in H_2O). Possible reasons for the lack of peak shift and the decreased intensity of the 528 nm band for HRP:Au include the larger size of HRP (~45 Å as compared to ~34 Å for Cc)[47] and poorer adsorption of conjugates to Ag aggregates: note that SERS attempts on HRP and HRP:Au at aggregated Ag were unsuccessful under conditions that gave rise to good spectra for Cc and Cc:Au (data not shown).[48−49]

The key point from the data in Figure 5 is that the optical properties of cytochrome *c*-coated colloidal Au nanoparticles are strongly perturbed by aggregated Ag. The magnitude of the perturbation, as manifested by the shift in λ_{max}, reflects the separation between the Au nanoparticles and the aggregated Ag substrate. Au particles lacking protein coating can contact Ag aggregates directly, and their optical spectra are perturbed more than Cc:Au.

Photoinduced Conformational Changes of Cc in Ag:Cc:Au. Strong additional evidence for wavelength-dependent coupling between aggregated Ag and Cc-coated Au is found by the presence (or absence) of photoinduced conformational changes in Cc. It has been convincingly demonstrated that substrates with large surface electromagnetic fields are enhancing not only for SERS but for a variety of photon-driven phenomena, including second-harmonic generation,[50] fluorescence,[51] and photochemistry.[52] For Cc at metal surfaces, the most likely photoinduced processes are conformational changes affecting the heme pocket, including spin state conversion; such changes are readily detectable by SERS. Thus, Cc molecules sandwiched between Au and Ag surfaces might be expected to show greater instability with respect to laser illumination than Cc bound only to the Ag surface. This is indeed the case: we find greater photosusceptibility for Ag:Cc:Au than for Ag:Cc using 568.2-nm excitation. However, at 514.5 nm, an excitation wavelength for which the colloidal Au particle is "turned off", and there is no difference in photostability between Ag:Cc:Au and Ag:Cc.

Figure 6 shows SERS spectra for Ag:Cc:Au (top part) and Ag:Cc (bottom part) immediately after sample preparation (curve a) and after samples were left in a ~50 mW, 568.2 nm beam for 30 min (curve b). Several changes can be seen in the Ag:Cc:Au spectra. After 30 min, the overall signal has grown,[53] and the relative intensities of the bands (particularly ν_{10}, ν_4) have altered noticeably. In addition, a new vibration at ~1626 cm^{-1} has appeared; the presence of this band indicates that some of the Fe has converted to a high spin state.[16] Overall, the spectral changes for Ag:Cc:Au indicate that there has been some change in the structure of adsorbed Cc. In contrast, no such

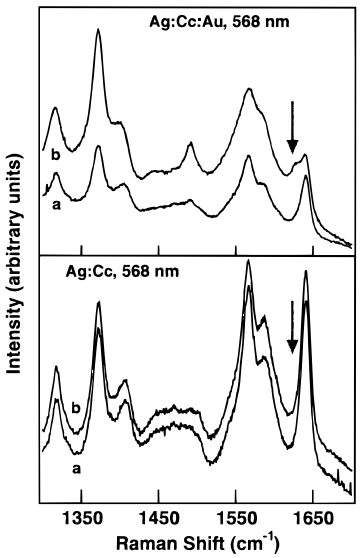

Figure 6. SERS spectra at 568.2-nm excitation for Cc:Au conjugates (top) and Cc (bottom) adsorbed to aggregated colloidal Ag. In each part, spectrum a was taken immediately after SERS sample preparation, and spectrum b after 30 min of irradiation with the ~50 mW, 568.2-nm beam. [Cc] $\sim 7.0 \times 10^{-7}$ M in these samples.

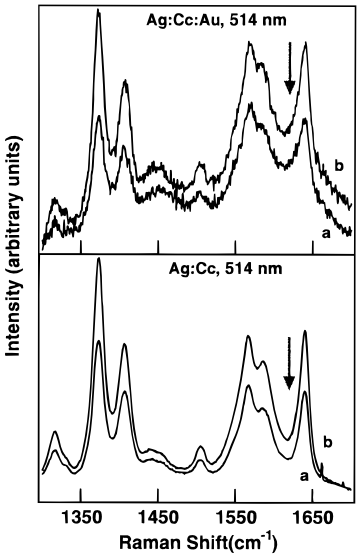

Figure 7. SERS spectra at 514.5-nm excitation for Cc:Au conjugates (top) and Cc (bottom) adsorbed to aggregated colloidal Ag. In each part, spectrum a was taken immediately after SERS sample preparation, and spectrum b after 30 min of irradiation with the ~50 mW 514.5-nm beam. [Cc] $\sim 6.8 \times 10^{-8}$ M.

changes are observed in the spectra of Ag:Cc at the same concentration (lower part). Hence, it appears that Cc adsorbed directly to Ag is more stable to photoinduced conformational changes than is Cc:Au at 568.2-nm excitation.[54]

If the increased susceptibility to irradiation for Cc:Au as compared to Cc is due to the increased EM field experienced by Cc located between Au particles, then it should not be observed at excitation wavelengths for which there is damping of the surface plasmon. Figure 7 shows SERS spectra for Cc:Au (top part) and Cc (bottom part) adsorbed to aggregated Ag before and after 30 min of irradiation with ~50 mW of 514.5-nm light. No evidence for spin state conversion or other conformational changes is observed in either sample. Thus, the changes observed in the Cc:Au spectra using 568.2-nm excitation can be attributed to the increased fields experienced by Cc molecules between Au nanoparticles and the surface of the Ag aggregates when both particles are "turned on".

CHART 2: "Squeezed Sandwich" Geometry

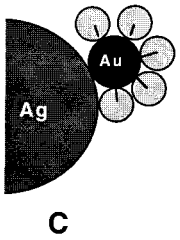

C

These data are critical not only for demonstrating the wavelength dependence of the electromagnetic coupling between the Ag and Au particles but also for ruling out alternative geometries for **B** in Chart 1. The most important of these is the "squeezed sandwich" geometry (**C**) of Chart 2, in which the Cc:Au conjugate is adsorbed to Ag, but with the Cc molecules that would be directly between the particles removed. Since none of the Cc molecules in geometry **C** are sandwiched between particles, they would not exhibit an increased EM field relative to **A** (i.e., directly adsorbed Cc), and consequently would not be expected to undergo a photoinduced spin-state conversion. That Ag:Cc:Au conjugates do so, but only at a wavelength where the colloidal Au particle contributes maximally to SERS, is compelling evidence against **C**.

Other Metal Nanoparticle:Cc:Metal Nanoparticle Sandwiches. Having established that 12-nm diameter Au nanoparticles are active in the enhancement of Cc Raman scattering from sandwiches of the form Ag:Cc:Au, it was of interest to determine whether this phenomenon was unique to these types of particles. Accordingly, we prepared five other metal particle:Cc:metal particle sandwiches: Ag:Cc:Ag/Au, Ag:Cc:Au(40), Ag:Cc:Au(60), Au:Cc:Au, and Ag:Cc:Ag. These systems have furthered our understanding of the electromagnetic coupling between particles.

As a first step, the optical and SERS behavior of conjugates prepared with Ag/Au were explored. These particles comprised a 12-nm diameter colloidal Au core with a 3-nm thick Ag cladding.[41] The addition of the Ag cladding dramatically alters the optical spectrum of the particles, with the Ag/Au particles exhibiting both Ag-like and Au-like surface plasmon bands (Supporting Information). SERS spectra were acquired at five excitation wavelengths for Ag:Cc:Ag/Au and compared to the corresponding spectra for Ag:Cc under identical conditions (Supporting Information). Once again, the latter yielded more intense spectra at all excitation wavelengths. The Supporting Information also contains a plot of ν_4 intensity ratio of Ag:Cc:Ag/Au to Ag:Cc vs excitation wavelength.[55] However, the data differed from that of Figure 4 in two major respects. First, the ν_4 intensity ratios peaked at > 0.5, as opposed to <0.4. Second, and more importantly, the data are nearly wavelength independent. Thus, while wavelength-dependent ν_4 intensity ratios vary for Ag:Cc:Au by a factor of 4, they only vary in Ag:Cc:Ag/Au by 50% or less (Supporting Information). In other words, at all excitation wavelengths, Cc and Cc:Ag/Au yield comparable SERS intensities upon adsorption to aggregated Ag. It is likely that the wavelength independence of these conjugates reflects wavelength-dependent contributions from both the Au core and the Ag cladding in different regions of the spectrum (vide infra).

Another approach to change the electromagnetic field between particles is to increase the size of the colloidal Au nanoparticle, which might be expected to increase signal.[3,29,34] Accordingly, conjugates were prepared using 40-nm and 60-nm Au nano-

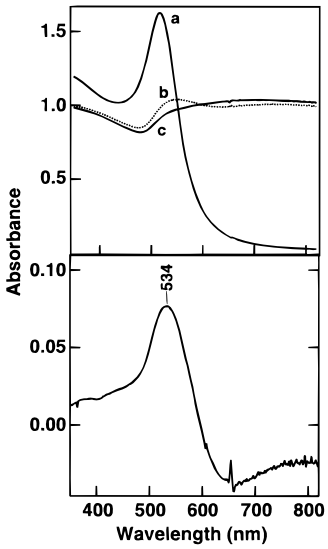

Figure 8. Top: Optical spectra for (curve a) unaggregated 12-nm colloidal Au, (curve b) SERS sample consisting of Cc:Au adsorbed to aggregated 12-nm colloidal Au, diluted 1:1 with H_2O; (curve c) SERS sample of Cc adsorbed to aggregated colloidal Au, diluted 1:1 with H_2O. Bottom: difference spectrum for b and c.

particles. The maximum for the surface plasmon absorbance occurs at 518 nm for conjugates prepared using 12-nm Au, at 534 nm for 40-nm Au, and at 538 nm for the 60-nm diameter Au particles (Supporting Information). Such particle size-dependent shifts in the position of λ_{max} are expected, and could affect the observed SERS signal from Cc:Au adsorbed at colloidal Ag aggregates. Since the ν_4 vibration at $\sim$1375 cm^{-1} is relatively insensitive to changes in Cc orientation (concentration),[12,56] it is therefore the best band to examine for comparison between Cc and Cc:Au intensities for the various conjugates. Such a comparison indicates that there is little dependence of scattering intensity on particle diameter (Supporting Information). While this result could be explained by an Au diameter-dependent field that is offset by size-dependent differences in the equilibrium constant for adsorption of Cc:Au, a more likely explanation is that the effects of size variations in one particle of a biospheroidal system are not expected to be significant as compared to the effects of location between particles, especially when the optical properties of the part of the sandwich that is varied (i.e., the Au) are quite similar.

More significant changes in SERS behavior have been found via preparation of sandwiches with the same metal (e.g., Au:Cc:Au and Ag:Cc:Ag). The top part of Figure 8 shows optical spectra for unaggregated 12-nm Au nanoparticles (trace a), aggregated 12-nm Au nanoparticles with adsorbed Cc:Au (trace b), and aggregated 12-nm Au nanoparticles with adsorbed Cc (trace c). The subtraction spectrum for spectrum b minus spectrum c is shown in the bottom part of Figure 8. The subtraction spectrum for Cc:Au on aggregated Au is similar to that for Cc:Au on aggregated Ag (Figure 5, bottom), except that the peak is shifted only $\sim$15 nm for the Au:Cc:Au, as compared to $>$50 nm for the Ag:Cc:Au sandwiches. This is consistent with the greater electromagnetic fields at the Ag aggregates relative to aggregates of 12-nm Au particles. SERS spectra for both Au:Cc:Au and Au:Cc at λ_{ex} = 514.5, 568.2, and 647.1 nm are shown in Figure 9. Due to weak SERS enhancement at Au aggregates as compared to Ag aggregates (even at long λ_{ex}), spectra exhibiting poor signal/noise ratios were obtained in all cases. No bands are observed in either Cc or Cc:Au SERS at Au aggregates for λ_{ex} = 514.5 nm. Very

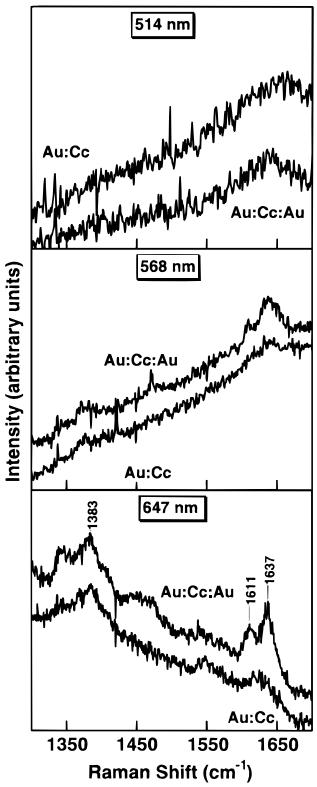

Figure 9. SERS spectra for Au:Cc and Au:Cc:Au at three excitation wavelengths. Conditions: 10-s integration $\times$ 10 accumulations for all wavelengths; 37 mW incident power at 514.5-nm excitation, 45 mW at 657.1 nm, and 50 mW at 568.2 nm.

weak bands due to Cc (at $\sim$1375 and $\sim$1635 cm^{-1}) are observed for λ_{ex} = 568.2 and 647.1 nm in both data sets. SERS signal from Cc:Au is slightly better than that from Cc under these conditions. The wavelength dependence of the SERS spectra in Figure 9 can be understood in terms of the effects of Au surface plasmon damping at short wavelengths, as for the corresponding system with Ag aggregates in place of Au aggregates. More importantly, the finding that the SERS intensity from Au:Cc:Au, although weak, exceeds that for Au:Cc reinforces the conclusion that the EM field strength between particles (in this case, Au) and aggregates is large compared to that surrounding Au aggregates.

This being the case, the most intense SERS spectra should arise through coupling of aggregated Ag and isolated Ag particles. To test this, Cc:Ag conjugates were prepared and characterized optically. Cc:Ag conjugates exhibit an absorbance maximum at 408 nm, and a weaker, broad shoulder extending out to nearly 700 nm (Figure 10, top part). The presence of a broad shoulder at longer wavelengths in the optical spectrum is indicative of some aggregation of the Ag particles in the solution. This feature in the optical spectrum was not present in the EDTA-reduced Ag sol, nor in the Cc:Ag conjugates prior to centrifugation. Indeed, the color of the conjugates was observed to change color rapidly form a bright, transparent yellow to a slightly cloudy, greenish yellow almost immediately upon resuspension of the conjugates. It is not possible to determine from the data here whether formation of aggregates results in entrapment of Cc molecules between Ag particles prior to exposure to the intentionally aggregated citrate-reduced Ag sol for SERS measurements, or whether Cc molecules have desorbed from the Cc:Ag conjugates, leading to the observed aggregate formation. In either case, the geometry in these

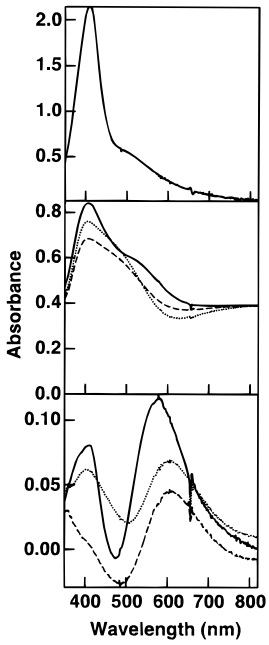

Figure 10. Top: optical spectrum of Cc:Ag conjugates, diluted 1:5 with H_2O. Middle: optical spectra for SERS samples consisting of aggregated Ag sol with added H_2O (•••), Cc (− − −), and Cc:Ag (—). Aggregated samples were prepared as described in the Experimental Section and then diluted 1:4.3 with H_2O. Bottom: Difference spectrum for Cc:Ag SERS sample minus the spectrum for the aggregated Ag sol (—), and for uncoated EDTA-reduced colloidal Ag added to citrate-reduced Ag sol before (− − −) and after (•••) aggregation induced by addition of NaCl.

samples upon exposure to aggregated Ag is that of Ag particles on either side of Cc molecules.

The absorbance spectrum for a Cc:Ag SERS sample (i.e., Ag:Cc:Ag) is shown in the middle part of Figure 10 (solid line), along with the spectra for SERS samples containing Cc and H_2O as analyte (each sample has aggregated Ag sol as substrate). Only the Ag:Cc:Ag sample has a shoulder ∼550 nm. This feature is due to a peak at ∼580 nm observable in the optical difference spectrum for this sample minus an aggregated Ag blank (Figure 10, bottom part, solid line). For comparison, difference spectra for uncoated EDTA-reduced Ag sol added to citrate-reduced Ag sol before (− − −) and after (•••) aggregation are also shown in the bottom part of Figure 10. Both difference spectra for uncoated Ag are qualitatively similar to that for Cc:Ag, except that the large feature is less intense and located further to the red (∼600 nm) for the uncoated Ag difference spectra. None of these difference spectra bears much resemblance to unaggregated EDTA-reduced Ag sol, or to Cc:Ag. Due to similarities in the absorbance spectra of, and greater EM coupling between, Ag aggregates and Cc-coated Ag nanoparticles (as compared to Cc-coated 12-nm Au), it is more difficult to separate the contribution of Cc:Ag from that of the bulk-aggregated Ag.

SERS spectra of Ag:Cc and Ag:Cc:Ag at five excitation wavelengths are presented in Figure 11. At each λ_{ex} shown, Ag:Cc:Ag spectra (solid lines) are *more* intense than Ag:Cc (dashed lines). Once again, it is important to point out that spectra were acquired with the same total [Cc], the same laser power and integration time (for a given λ_{ex}), and for identically prepared samples. This shows that enhancement due to location between the Ag nanoparticle of the conjugate and the Ag aggregate more than compensates for the decrease in signal caused by the longer distance between the Ag aggregates and the Cc heme group. Unlike the Cc:Au conjugates, Cc:Ag

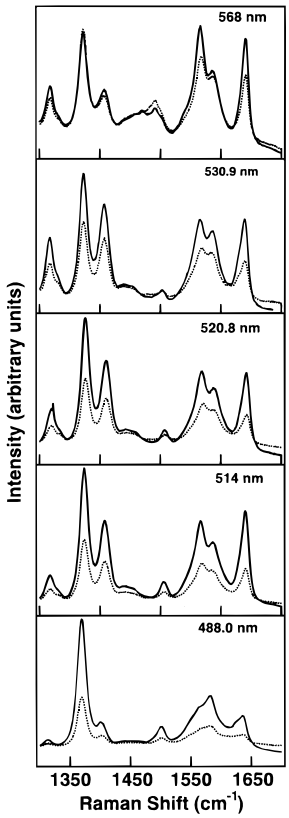

Figure 11. SERS spectra at for Ag:Cc:Ag (—) and Ag:Cc (•••) at (from top to bottom) the following excitation wavelengths (laser powers, integration times): 568.2 nm (57 mW, 30 s), 530.9 nm (43 mW, 30 s), 520.8 nm (47 mW, 15 s), 514.5 nm (53 mW, 30 s), and 488.0 nm (130 mW, 5 s). [Cc] = 3.2×10^{-8} M. Each spectrum shown is the average of three accumulations for the same sample.

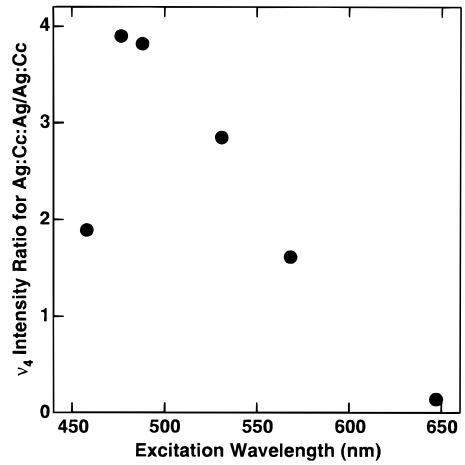

Figure 12. ν_4 intensity ratio of Ag:Cc:Ag to Ag:Cc vs excitation wavelength.

conjugates give optimal SERS at shorter λ_{ex}. A plot of the ν_4 intensity ratio of Ag:Cc:Ag/Ag:Cc vs λ_{ex} is shown in Figure 12. Not surprisingly, the maximal benefits of Cc:Ag conjugates are realized at shorter excitation wavelengths; for example, at 488.0 nm, the ν_4 intensity of Cc:Ag adsorbed at aggregated Ag is four times that of directly adsorbed Cc. Considering how few of the Cc molecules are actually sandwiched, this is an impressive increase. At the very least, it offers a practical prescription for increased SERS intensities in experiments involving proteins.

A final interesting aspect to the data in Figure 12 is the significantly reduced intensity of the conjugates relative to free

Cc at $\lambda_{ex} = 647.1$ nm. Since the Ag surface plasmon is not damped at any of the wavelengths in the visible spectrum, this result introduces the possibility that electronic coupling between metal particles might be mediated by the (resonant) electronic properties of the heme; that is, coupling is only strong at wavelengths where the heme extinction is (even slightly) nonzero. An alternate explanation is that what is being interrogated in these experiments are microenvironments that respond differently at different excitation wavelengths. Such an explanation is consistent both with theory[34] and recent experiments.[29,30]

Conclusions

A wealth of data indicates the presence of heightened electromagnetic fields between metal nanoparticles. These include (a) wavelength-dependent SERS spectral intensities for Ag:Cc:Au relative to Ag:Cc, (b) a dramatically redshifted single particle surface plasmon band for Au in Ag:Cc:Au, (c) increased SERS intensities for Au:Cc:Au relative to Au:Cc and for Ag:Cc:Ag relative to Ag:Cc, and (d) a wavelength-dependent photoinduced conformational change in Ag:Cc:Au that is not observed for Ag:Cc. The ability to prepare analyte:metal particle conjugates that allow precise positioning of the analyte between metal particles creates numerous new possibilities for SERS of biomolecules, both from fundamenatal and applied perspectives. Moreover, these studies pave the way for detailed experimental tests of theoretically predicted electromagnetic effects between closely spaced metal particles.

Acknowledgment. We are indebted to Ken Brown for chromatographic purification of horse heart cytochrome *c*, and to Prof. W. DeW. Horrocks and his research group for the use of the microcentrifuge. Support from NSF (Grant CHE-9627338), NIH (Grants GM55312-01 and DK48784-01A2), and the Henkel Corporation/ACS Division of Colloid and Surface Chemistry (through a graduate fellowship to C.D.K.) is gratefully acknowledged. Acknowledgment is also made to the Electron Microscopy Facility for the Life Sciences in the Biotechnology Institute at The Pennsylvania State University. K.M.K. thanks the Penn State Chemistry Department for a Teas Fellowship, and M.J.N. thanks George Schatz, Martin Moskovits, and Richard Van Duyne for helpful discussions.

Supporting Information Available: Raman spectrum for concentrated Cc:Au at $\lambda_{ex} = 568.2$ nm, SERS spectra for Ag:Cc:Au and Ag:Cc at 514.5-, 520.8-, 530.9-, and 568.2-nm excitation wavelengths, optical spectrum for Ag/Au particles, SERS spectra and ν_4 ratio plot for Ag:Cc:Ag/Au vs Ag:Cc; optical spectra for 12-, 40-, and 60-nm diameter colloidal Au particles, and SERS spectra for Ag:Cc:Au(12), Ag:Cc:Au(40), and Ag:Cc:Au(60) each vs Ag:Cc (10 pages total). Ordering information is given on any current masthead page.

References and Notes

(1) (a) Brandt, E. S.; Cotton, T. M. In *Investigations of Surfaces and Interfaces-Part B*, 2nd ed.; Rossiter B. W., Baetzold R. C., Eds.; John Wiley & Sons: New York, 1993; Chapter 8. (b) Garrell, R. L. *Anal. Chem.* **1989**, *61*, 410A-411A. (c) Campion, A. In *Vibrational Spectroscopy of Molecules on Surfaces;* Yates, J. T., Jr., Madley, T. E. M., Eds.; Plenum: New York, 1987; pp 345−415.

(2) Jeanmaire, D. L.; Van Duyne, R. P. *J. Electroanal. Chem.* **1977**, *84*, 1−20.

(3) Schatz, G. C. *Acc. Chem. Res.* **1984**, *17*, 370−376.

(4) (a) Campion, A.; Ivanecky III, J. E.; Child, C. M.; Foster, M. *J. Am. Chem. Soc.* **1995**, *117*, 11807−11808. (b) Kambhampati, P.; Child, C. M.; Campion, A. *J. Chem. Soc., Faraday Trans.* **1996**, *92*, 4775−4780.

(5) Otto, A.; Mrozek, I.; Grabhorn, H.; Akemann, W. *J. Phys. Condens. Matter* **1992**, *4*, 1143−1212.

(6) (a) Barz, F.; Gordon, J. G., II; Philpott, M. R.; Weaver, M. J. *Chem. Phys. Lett.* **1983**, *94*, 168−171. (b) Wolkow, R. A.; Moskovits, M. *J. Chem. Phys.* **1992**, *96*, 3966−3980. (c) Gu, X. J.; Akers, K. L.; Moskovits, M. *J. Phys. Chem.* **1991**, *95*, 3696−3700. (d) Kannen, G.; Otto, A. *Chem. Phys.* **1990**, *141*, 51−61. (e) Beer, K. D.; Tanner, W.; Garrell, R. L. *J. Electroanal. Chem.* **1989**, *258*, 313−325.

(7) (a) Osawa, M.; Yamamoto, S.; Suetaka, W. *Appl. Surf. Sci.* **1988**, *33/34*, 890−897. (b) Albano, E. V.; Daiser, S.; Ertl, G.; Miranda, R.; Wandelt. K.; Garcia, N. *Phys. Rev. Lett.* **1983**, *51*, 2314−2317.

(8) Liver, N.; Nitzan, A.; Gersten, J. I. *Chem. Phys. Lett.* **1984**, *111*, 449−454.

(9) (a) Sestak, O.; Matejka, P.; Vlckova, B. *Collect. Czech. Chem. Commun.* **1996**, *61*, 59−69. (b) Xu, M.; Dignam, M. J. *J. Chem. Phys.* **1994**, *100*, 197−203. (c) Inoue, M.; Ohtaka, K. *J. Phys. Soc. Jpn.* **1983**, *52*, 3853−3864. (d) Barber, P. W.; Chang, R. K.; Massoudi, H. *Phys. Rev. B* **1983**, *27*, 7251−7261.

(10) (a) Hayat M. A., Ed. *Colloidal Gold: Principles, Methods, and Applications*; Academic Press: New York, 1989 (in three volumes). (b) Polak, J. M., Van Noorden, S., Eds. *Immunocytochemistry*; Wright: London, 1983.

(11) Keating, C. D.; Kovaleski, K. M.; Natan, M. J. *J. Phys. Chem. B* **1998**, *102*, 9404.

(12) (a) De Roe, C.; Courtoy, P. J.; Baudhuin, P. *J. Histochem. Cytochem.* **1987**, *35*, 1191−1198. (b) Geoghegan, W. D.; Ackerman, G. A.; *J. Histochem. Cytochem.* **1977**, *25*, 1187−1200. (c) Horisberger, M. *Biol. Cell.* **1979**, *36*, 253.

(13) Ahern, A. M.; Garrell, R. L. *Langmuir* **1991**, *7*, 254−261

(14) (a) Elghanian, R.; Storhoff, J. J.; Mucic, R. C.; Letsinger, R. L.; Mirkin, C. A. *Science* **1997**, *277*, 1078−1081. (b) Mirkin, C. A.; Letsinger, R. L.; Mucic, R. C.; Storhoff, J. J. *Nature* **1996**, *382*, 607−609.

(15) (a) Scott, R. A., Mauk, A. G., Eds. *Cytochrome c: A Multidisciplinary Approach*; University Science Books: Sausalito, CA, 1996. (b) Lever, A. B. P., Gray, H. B., Eds. *Iron Porphyrins*; Addison-Wesley: Reading, MA, 1983 (in two volumes). (c) Moore, G. R., Pettigrew, G. W., Eds. *Cytochromes c: Evolutionary, Structural and Physicochemical Aspects*; Springer-Verlag: Berlin, 1990.

(16) (a) Spiro, T. G., Ed. *Biological Applications of Raman Spectroscopy*; John Wiley & Sons: New York, 1988; Vol. 3. (b) Hildebrandt, P. In *Cytochrome c: A Multidisciplinary Approach*; Scott, R. A., Mauk, A. G., Eds. University Science Books: Sausalito, CA, 1996, Chapter 6. (c) Cartling, B. *Biophys. J.* **1983**, *43*, 191−205.

(17) MacDonald, I. D. G.; Smith, W. E. *Langmuir* **1996**, *12*, 706−713.

(18) (a) Hildebrandt, P.; Stockburger, M. *Biochemistry* **1989**, *28*, 6710−6721. (b) Hildebrandt, P.; Stockburger, M. *Biochemistry* **1989**, *28*, 6722−6728. (c) Hildebrandt, P.; Stockburger, M. *J. Phys. Chem.* **1986**, *90*, 6017−6024. (d) Hildebrandt, P.; Stockburger, M. *J. Phys. Chem.* **1986**, *90*, 6017−6024.

(19) (a) Sibbald, M. S.; Chumanov, G.; Cotton, T. M. *J. Phys. Chem.* **1996**, *100*, 4672−4678. (b) Niaura, G.; Gaigalas, A. K.; Vilker, V. L. *J. Electroanal. Chem.* **1996**, *416*, 167−178. (c) Maeda, Y.; Yamamoto, H.; Kitano, H. *J. Phys. Chem.* **1995**, *99*, 4837−4841. (d) Hobara, D.; Niki, K.; Zhou, C.; Chumanov, G.; Cotton, T. M. *Colloids Surf., A* **1994**, *93*, 241−250. (e) Cotton, T. M.; Schultz, S. G.; Van Duyne, R. P. *J. Am. Chem. Soc.* **1980**, *102*, 7962−7965.

(20) (a) Edmiston, P. L.; Lee, J. E.; Cheng, S.-S., Saavedra, S. S. *J. Am. Chem. Soc.* **1997**, *119*, 560−570. (b) Lee, J. E.; Saavedra, S. S. *Langmuir* **1996**, *12*, 4025−4032. (c) Heimburg, T.; Hildebrandt, P.; Marsh, D. *Biochemistry* **1991**, *30*, 9084−9089. (d) Hildebrandt, P. *J. Mol. Struct.* **1991**, *242*, 379−395.

(21) (a) Ye, Q.; Fang, J.; Sun, L. *J. Phys. Chem. B* **1997**, *101*, 8221−8224. (b) Tsen, M.; Sun, L. *Anal. Chim. Acta* **1995**, *307*, 333−340.

(22) (a) Cotton, T. M.; Uphaus, R. A.; Mobius, D. *J. Phys. Chem.* **1986**, *90*, 6071−6073. (b) Kovacs, G. J.; Luotfy, R. O.; Vincett, P. S.; Jennings, C.; Aroca, R. *Langmuir* **1986**, *2*, 689−694.

(23) (a) Murray, C. A.; Allara, D. L. *J. Chem. Phys.* **1982**, *76*, 1290−1303. (b) Murray, C. A.; Allara, D. L.; Rhinewine, M. *Phys. Rev. Lett.* **1981**, *46*, 57−60.

(24) Heard, S. M.; Greieser, F. J.; Barraclough, C. G. *J. Colloid Interface Sci.* **1983**, *93*, 545−555.

(25) (a) Creighton, J. A. In *Spectroscopy of Surfaces;* Clark, R. J., Hester, R. P., Eds. Wiley: New York, 1988; 37−89. (b) Moskovits, M. *J. Chem. Phys.* **1982**, *77*, 4408−4416.

(26) Broderick, J. B.; Natan, M. J.; O'Halloran, T. V.; Van Duyne, R. P. *Biochemistry* **1993**, *32*, 13771−13776.

(27) Rospendowski, B. N.; Kelly, K.; Wolf, C. R.; Smith, W. E. *J. Am. Chem. Soc.* **1991**, *113*, 1217−1225.

(28) In the M:Cc:M notation, the metal to the left of the "Cc" always refers to the aggregated colloidal substrate and that on the right to the Cc-coated metal nanoparticle. For example, Ag:Cc:Au refers to Cc:Au nanoparticle conjugates adsorbed at the surface of aggregated colloidal Ag.

(29) (a) Emory, S. R.; Nie, S. *Science* **1997**, *275*, 1102−1106. (b) Emory, S. R.; Nie, S. *Anal. Chem.* **1997**, *69*, 2631−2635.
(30) Kneipp, K.; Wang, Y.; Kneipp, H.; Perelman, L. T.; Itzkan, I.; Dasari, R. R.; Feld, M. S. *Phys. Rev. Lett*. **1997**, *78*, 1667−1670.
(31) Bright, R. M.; Musick, M. D.; Natan, M. J. *Langmuir* **1998**, *14*, 5695−5701.
(32) Frens, G. *Nature Phys. Sci.* **1973**, *241*, 20−22.
(33) Grabar, K. C.; Freeman, R. G.; Hommer, M. B.; Natan, M. J. *Anal. Chem.* **1995**, *267*, 1629−1632.
(34) Zeman, E. J.; Schatz, G. C. *J. Phys. Chem.* **1987**, *91*, 634−643.
(35) Nakamoto, K. *Infrared and Raman Spectra of Inorganic and Coordination Compounds*, 4th ed.; Wiley: New York, 1986.
(36) (a) Sanchez-Cortes, S.; Garcia-Ramos, J. V.; Morcillo, G. *J. Colloid Interface Sci.* **1994**, *167*, 428−436. (b) Quinten, M.; Kreibig, U. *Surf. Sci*. **1986**, *172*, 557−577. (c) Kreibig, U.; Vollmer, M. *Optical Properties of Metal Clusters*; Toennies, J. P., Ed.; Springer-Verlag: Berlin, 1995.
(37) (a) Blatchford, C. G.; Campbell, J. R.; Creighton, J. A. *Surf. Sci.* **1982**, *120*, 435−455. (b) Pockrand, I. *Chem. Phys. Lett*. **1982**, *85*, 37−42.
(38) Brautigan, D. L.; Ferguson-Miller, S.; Margoliash, E. *Methods Enzymol*. **1978**, *53*, 128−164.
(39) Lee, P. V.; Meisel, D. *J. Phys. Chem*. **1982**, *86*, 3391−3395.
(40) (a) Schutt, E. G. Eur. Pat. Appl. 90317671.4, September 25, 1990. (b) Brown, K. R.; Natan, M. J. *Langmuir* **1998**, *14*, 726−728.
(41) Freeman, R. G.; Hommer, M. B.; Grabar, K. C.; Jackson, M. A.; Natan, M. J. *J. Phys. Chem*. **1996**, *100*, 718−724.
(42) (a) Sanchez-Cortez, S.; Garcia-Ramos, J. V.; Morcillo, G. J. *Colloid Interface Sci*. **1994**, *167*, 428−436. (b) Sanchez-Cortez, S.; Garcia-Ramos, J. V.; Morcillo, G. J.; Tinti, A. *Colloid Interface Sci.* **1995**, *175*, 358−368. (c) Feilchenfeld, H.; Siiman, O. *J. Phys. Chem*. **1986**, *90*, 4590−4599. (d) Weitz, D. A.; Oliveria, M. *Phys. Rev. Lett.* **1984**, *52*, 1433−1436.
(43) Actually, type **A** samples are expected to contain 10% more Cc than type **B**, since the excess Cc in Cc:Au conjugates was removed in the centrifugation/resuspension step.
(44) Sanchez, L. A.; Spiro, T. G. *J. Phys. Chem*. **1985**, *89*, 763−768.
(45) (a) Shelnutt, J. A.; Cheung, L. D.; Chang, R. C. C.; Yu, N.-T.; Felton, R. H. *J. Chem. Phys*. **1977**, *66*, 3387−3398. (b) Shelnutt, J. A.; O'Shea, D. C.; Yu, N.-T.; Cheung, L. D.; Felton, R. H. *J. Chem. Phys*. **1976**, *64*, 1156−1165.
(46) Bushnell, G. W.; Louie, G. V.; Breyer, G. D. *J. Mol. Biol.* **1990**, *214*, 585−595.
(47) Brown, K. R. Thesis, The Pennsylvania State University, University Park, PA, 1997.
(48) Note that others (see ref 49) have observed SERS for HRP at Ag surfaces under different conditions (including several orders of magnitude higher protein concentrations).
(49) Silin, V. I.; Talaikyte, Z.; Kulys, J. *Vib. Spectrosc*. **1993**, *5*, 345−351.
(50) (a) Bavli, R.; Yogev, D.; Efrima, S.; Berkovic, G. *J. Phys. Chem*. **1991**, *95*, 7422−7426. (b) Johnson, C. K.; Soper, S. A. *J. Phys. Chem*. **1989**, *93*, 7281−7285. (c) Chen, C. K.; Heinz, T. F.; Ricard, D.; Shen, Y. R. *Phys. Rev. B* **1983**, *27*, 1965−1979. (d) Chen, C. K.; de Castro, A. R. B.; Shen, Y. R. *Phys. Rev. Lett*. **1981**, *46*, 145−148.
(51) (a) Glass, A. M.; Liao, P. F.; Bergman, J. G.; Olson, D. H. *Opt. Lett*. **1980**, *5*, 368−370. (b) Ritchie, G.; Burstein, E. *Phys. Rev. B* **1981**, *24*, 4843−4846.
(52) (a) Vlckova, B.; Gu, X. J.; Moskovits, M. J. *Phys. Chem. B* **1997**, *101*, 1588−1593. (b) Vlckova, B.; Gu, X. J.; Tsai, D. P.; Moskovits, M. *J. Phys. Chem*. **1996**, *100*, 3169−3174. (c) Suh, J. S.; Jang, N. H.; Jeong, D. H.; Moskovits, M. *J. Phys. Chem*. **1996**, *100*, 805−813. (d) Nitzan, A.; Brus, L. E. *J. Chem. Phys*. **1981**, *74*, 5321−5322. (e) Nitzan, A.; Brus, L. E. *J. Chem. Phys*. **1981**, *75*, 2205−2214.
(53) Increased intensities observed for SERS samples after 30 min irradiation are most likely due to changes in the aggregation state of the samples, leading to improved enhancement.
(54) Note, however, that the irradiation time required to see these changes far exceeds that needed to acquire a SERS spectrum and that no attempts were made to cool or mix samples during irradiation.
(55) Note that this intensity ratio is the inverse of that described in Figure 3; for the remainder of the manuscript all ratios will follow the convention of conjugate/Cc, for more facile comparison to optical spectra.
(56) The angle between the heme and the substrate is dependent upon the [Cc] (see ref 16), which varies with particle size as a result of differences in particle concentration. The band at ∼1640 cm^{-1} (ν_{10}) is more sensitive to this angle than is the band ∼1375 cm^{-1} (ν_4), due to symmetry considerations. For a more complete discussion of Cc orientation at colloidal particles, refer to the preceding article.